

Human-Object Interaction with Vision-Language Model Guided Relative Movement Dynamics

Zekai Deng¹ Ye Shi¹ Kaiyang Ji¹ Lan Xu¹ Shaoli Huang² Jingya Wang^{1†}
¹ShanghaiTech University ²Astribot



Figure 1. Our Relative Movement Dynamics (RMD) architecture enables dynamic object interaction and long-term multi-task completion based on VLM guidance. RMD enables the automatic construction of a unified reward function applicable to various reinforcement learning interaction tasks.

Abstract

Human-Object Interaction (HOI) is vital for advancing simulation, animation, and robotics, enabling the generation of long-term, physically plausible motions in 3D environments. However, existing methods often fall short of achieving physics realism and supporting diverse types of interactions. To address these challenges, this paper introduces a unified Human-Object Interaction framework that provides unified control over interactions with static scenes and dynamic objects using language commands. The interactions between human and object parts can always be described as the continuous stable Relative Movement Dynamics (RMD) between human and object parts. By leveraging the world knowledge and scene perception capabilities of Vision-Language Models (VLMs), we translate language commands into RMD diagrams, which are used to guide goal-conditioned reinforcement learning for sequential interaction with objects. Our framework supports long-horizon interactions among dynamic, articulated, and static objects. To support the training and evaluation of

our framework, we present a new dataset named Interplay, which includes multi-round task plans generated by VLMs, covering both static and dynamic HOI tasks. Extensive experiments demonstrate that our proposed framework can effectively handle a wide range of HOI tasks, showcasing its ability to maintain long-term, multi-round transitions. For more details, please refer to our project webpage: <https://rmd-hoi.github.io/>.

1. Introduction

Human-Object Interaction (HOI) is pivotal for progress in fields like simulation, animation and robotics. The key research goal is to generate long-term, physically plausible human motions with corresponding object movements. Existing kinematic-based data-driven approaches [24, 62–64] often struggle with artifacts and lack of realism, as they depend on static or pre-defined object trajectories that fail to capture the nuanced, interactive dynamics between humans and moving objects.

	Methods	Dynamic Object	Articulated Object	Automated Reward Design	Long-horizon Transition	HOI Goal Definition	Multitask
Kinematic	NSM [30]	✓			✓	-	✓
	SAMP [8]					-	✓
	SceneDiffuser [11]					-	✓
	OMOMO [14]	✓				-	✓
Physics-Based	InterPhys [9]	✓				One-to-One	
	PhysHOI [40]	✓				Multi-to-Multi	
	UniHSI [45]			✓	✓	One-to-One	✓
	RMD (Ours)	✓	✓	✓	✓	Multi-to-Multi	✓

Table 1. **Comparative Analysis of Key Features between RMD and Other Methods.** The proposed framework enables a unified and automated design of goal states and reward functions. Additionally, the framework facilitates fine-grained modeling of spatio-temporal human-object interactions, ensuring natural and continuous interactions with static, dynamic, and articulated objects.

Alternatively, some recent works employ physics engines [21, 37] to create interactive environments where agents can learn interaction skills through goal-conditioned reinforcement learning [9, 27, 40, 41, 56]. These methods take advantage of the physical realism provided by simulations to train agents in a variety of tasks, resulting in more plausible motion sequences. However, existing works primarily focus on specific task designs (e.g., sitting [3, 57] or carrying [4, 7, 33, 50]), which introduces two main issues: 1) Various interaction tasks require carefully crafted, task-specific rewards designed by human experts. Due to the complexity of dynamic human-object interactions, these reward functions are extremely challenging to design [32]; 2) These task-specific training approaches require separate policy networks and struggle with long-horizon, multi-round transitions, as the sparse goal settings often leave agents in unrecoverable states for subsequent skill transitions.

Recent efforts, such as Eureka [20], have attempted to address the first issue by leveraging large language models to automate reward design and reveal latent reward structures beyond human intuition. However, the rewards generated in this manner frequently lack interpretability and do not align well with human perceptual cues, often resulting in unnatural, non-human-like motion. UniHSI [45] proposed a “chain of contacts” framework leveraging the power of Large Language Models. However, this framework focuses on “contact” as an instantaneous spatial relationship, neglecting the temporal dynamics with objects, thus making it unsuitable for handling dynamic and complex interaction tasks. Moreover, this point-goal-reaching formulation fails to fully account for the coordination of whole-body movements, resulting in suboptimal behaviors that lack the natural fluidity and human-like motion essential for realistic interactions.

Inspired by the concept of relative motion in classical mechanics [53], we propose a novel approach that models complex HOI as stable, relative movements between human and object parts. For example, when picking up a box, different body parts maintain consistent relative distances to

specific points on the object, capturing not only moment-to-moment goals (e.g., approaching the box) but also transitional behaviors (e.g., moving the box with both hands). This relational constraint encapsulates the spatial, temporal, and combinatorial elements of dynamic HOI, allowing for smoother and more realistic interactions. We introduce a bipartite diagram named the *Relative Movement Dynamics* (RMD) to describe the spatial-temporal relationships between human parts and object parts during a sub-sequence. Benefiting from the rapid development of Vision-Language Models (VLMs) and their powerful capabilities in world knowledge, we utilize a VLM as a high-level Planner to perceive the surrounding scene and decouple text instructions into sub-sequences, automatically formatting sub-motions into the RMD bipartite diagram. Accordingly, RMD is then constructed as the target in the goal-conditioned reinforcement learning. In summary, our contributions include:

- We propose a general physics-based HOI synthesis framework leveraging the powerful world knowledge of VLMs, supporting long-term interactions with a diverse range of objects, including static, dynamic and articulated ones.
- We introduce *Relative Movement Dynamics* (RMD), a spatial-temporal bipartite diagram designed to model fine-grained, complex dynamic interactions. RMD enables the automatic construction of a unified reward function applicable to various reinforcement learning interaction tasks.
- We create Interplay, a novel dataset including thousands of interaction plans with both static and dynamic interaction tasks. Extensive simulation results demonstrate the effectiveness of our approach.

2. Related Work

2.1. Human Motion Synthesis with Static Scenes

In the field of character animation and motion synthesis, most research has focused on human motion interacting with static 3D scenes [16, 51, 56, 59]. Typically, researchers break down complex instructions into several key

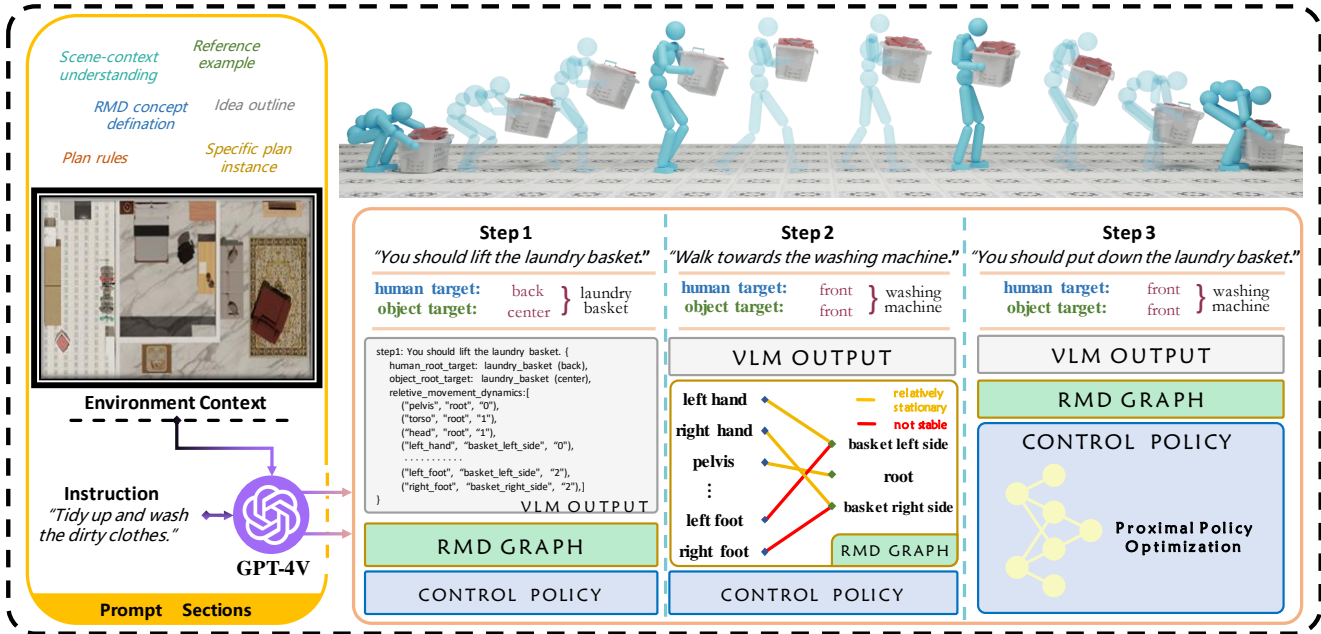


Figure 2. An overview of the concept of Relative Movement Dynamics and VLM-guided RMD Planner. RMD describes the spatial-temporal relationships between human parts and objects during a sub-sequence. We utilize a bipartite graph to formulate RMD, where each node corresponding to a human body part is uniquely connected to a node representing an object part. The edges in this graph encode the relative movement dynamics between the parts.

static poses within the scene [8, 39], and then use motion inpainting and optimization techniques to generate transitions between these key poses [38]. However, this approach often leads to mediocre and inconsistent motions due to the limited expressiveness of the intermediate sequences. Recently, diffusion-based methods like [10, 11, 34, 36, 52, 61] have achieved better results in human-scene synthesis. However, these data-driven approaches are limited to generating short-term motions due to constraints in the dataset, and the physical plausibility of the generated motions is not guaranteed. Apart from data-driven kinematic approaches, some studies have explored the problem within a reinforcement learning framework. For instance, [58, 60] achieved long-term goal-oriented behaviors by leveraging motion primitives with specific reward designs. The UniHSI [45] framework decomposes instructions into a sequence of point-reaching control tasks under a unified formulation. However, it addresses only the spatial constraints of static scenes while overlooking the temporal dynamics of objects, rendering it inadequate for managing complex dynamic interactions.

2.2. Kinematic-based Human Motion Synthesis with Dynamic Objects

Research in human motion synthesis has increasingly focused on modeling interactions with dynamic objects [12, 31, 54, 57]. Diffusion-based frameworks [14, 15, 25, 28],

guide motion generation with object trajectories but often lack realism due to predefined object paths that fail to account for physical plausibility. In contrast, InterDreamer [48] first generates human motion and subsequently uses a pre-trained world model to produce object trajectories, though this approach is limited by the simplicity of the world model, leading to inaccuracies in trajectory prediction. Some studies attempt to address these limitations by jointly modeling human-object interactions with supplementary guidance techniques, including relation intervention [42], contact prediction [5], and affordance estimation [25]. Truman [13], trained on a high-quality human-scene interaction (HSI) dataset, achieves dynamic stability through an auto-regressive diffusion model guided by action labels and waypoints. Nevertheless, kinematic models continue to face challenges such as penetration, sliding issues, and difficulties in generating long-term motion, requiring extensive annotations.

2.3. Physics-based Human Motion Synthesis with Dynamic Objects

To generate physically plausible motions, reinforcement learning methods have proven effective in training human-object interaction skills based on motion capture data [3, 22, 26, 43, 47, 49]. AMP [27] introduced an adversarial motion prior framework for realistic motion synthesis. InterPhys [9] further extended this framework by incorporat-

ing an HOI motion prior, achieving success in tasks such as sitting, lying, and carrying. Further advancements have led to successful applications in sports activities, including basketball [40, 41], tennis [55], soccer [46], skating [17], and football [18, 19]. Since these approaches often depend on heuristic designs and struggle to generalize to longer, multi-round scenarios. Our method seeks to address these limitations by introducing a Relative Movement Dynamics representation, enabling the model to capture both spatial and temporal dynamics effectively. This results in physically plausible and temporally coherent interactions, eliminating the need for manual annotations and enhancing realism in dynamic, long-term HOI tasks. The detailed comparisons of key features are listed in Tab. 1.

3. Method

In the following subsections, we first illustrate the concept of the proposed Relative Movement Dynamics (Sec. 3.1). Then, we demonstrate how we use VLM to perceive the scene context and decouple the text instruction into a plan in the form of RMD (Sec. 3.2). Finally, we elaborate on the construction of the RMD controller, which receives RMD plans as input and executes them step by step (Sec. 3.3).

3.1. Relative Movement Dynamics

Complex human-object interaction (HOI) tasks can be decomposed into several sub-sequences, where each human part maintains a consistent relative movement trend with its corresponding object part until the transition to the next sub-sequence. Therefore, we universally define the objective of the interaction plan as D , with the formulation as,

$$D = \{\mathcal{G}_0, \mathcal{G}_1, \dots, \mathcal{G}_m\}, \quad (1)$$

where \mathcal{G}_i denotes the i -th plan interaction step. \mathcal{G} is composed with three parts: the target location for human root, the target location for object root and the planned Relative Movement Dynamics between human parts and object parts, with the formulation as,

$$\mathcal{G} = \{\mathcal{T}_H, \mathcal{B}, \mathcal{T}_O\}, \quad (2)$$

\mathcal{B} is a bipartite graph, where each node corresponding to a human body part is uniquely connected to a node representing an object part. The edges in this graph encode the relative movement dynamics between the parts. In this context, we assume that the human body consists of 15 parts, while the object consists of k parts. In this way, we can formulate each \mathcal{B} as,

$$\mathcal{B} = \{e_{ij} \mid p_{h_i} \in P_H, p_{o_j} \in P_O, w_{ij} \in \{0, 1, 2, 3\}\}, \quad (3)$$

where P_H and P_O are the sets of human body parts and object parts, respectively. The set of human body parts is given by,

$$P_H = \{p_{h_1}, \dots, p_{h_{15}}\}, \quad (4)$$

The set of object parts is,

$$P_O = \{p_{o_1}, \dots, p_{o_k}\}, \quad (5)$$

Each edge $e_{ij} \in \mathcal{B}$ connects a human part $p_{h_i} \in P_H$ to an object part $p_{o_j} \in P_O$, with an edge weight w_{ij} representing the state of relative movement dynamics between the two parts. The interpretation of the weights is as follows,

- $w_{ij} = 0$ indicates that p_{h_i} and p_{o_j} remain relatively stationary with respect to each other during this period.
- $w_{ij} = 1$ indicates that p_{h_i} and p_{o_j} are moving towards each other during this period.
- $w_{ij} = 2$ indicates that p_{h_i} and p_{o_j} are moving away from each other during this period.
- $w_{ij} = 3$ indicates that p_{h_i} and p_{o_j} do not maintain a stable relative motion trend during this period.

3.2. VLM-guided RMD Planner

We utilize GPT-4v [1] as our planner to infer the spatial-temporal relationships between humans and objects during interactions in specific contexts. The planner translates high-level language commands \mathcal{L} into detailed plans D . As illustrated in Fig. 2, the RMD planner takes three main inputs: a language command \mathcal{L} , a top-view image representing the environmental context \mathcal{C} , and pre-defined prompts. Leveraging GPT-4v’s [1] vision capabilities, the RMD planner perceives the surrounding environment, identifies relevant objects, and infers their parts. To facilitate this process, we employ prompt engineering to ensure that GPT-4v [1] generates structured JSON documents, which can be easily encoded. By modifying both the instructions and the environment layout, we can generate diverse sequential interactions involving both static and dynamic objects. This approach allows us to create interaction datasets for evaluation, as detailed in the experiment section.

3.3. Policy Learning via RMD

Receiving the detailed plan output by the RMD Planner and background scenarios in the form of meshes and point clouds as input, the policy outputs specific torque for each joint to activate the agent and sequentially execute the plan. We begin by introducing the preliminaries of our method. Then, we describe the detailed formulation of the policy, including how the plan is translated into the goal state and how we construct the corresponding reward to encourage the agent to perform actions that align with the goal expectations.

Preliminary. Our physics-based animation framework is built upon goal-conditioned reinforcement learning. At each time step t , the agent samples an action from its policy $\pi(a_t \mid \mathbf{s}_t, \mathbf{g}_t)$ based on the current state \mathbf{s}_t and the goal state \mathbf{g}_t . After executing the action, the environment transitions to the next state \mathbf{s}_{t+1} , and the agent receives a task reward

$r^G(\mathbf{s}_t, \mathbf{g}_t, \mathbf{s}_{t+1})$. To train control policies that enable characters to perform high-level tasks in a natural and life-like manner, we adopt the AMP framework [27], which introduces a discriminator to encourage the character to produce behaviors similar to those in the dataset by providing a style reward $r^S(\mathbf{s}_t, \mathbf{s}_{t+1})$. Combining these two reward terms, the total reward at time step t is,

$$r_t = w^G r^G(\mathbf{s}_t, \mathbf{g}_t, \mathbf{s}_{t+1}) + w^S r^S(\mathbf{s}_t, \mathbf{s}_{t+1}). \quad (6)$$

Note that AMP, as well as most previous methods, spends time designing the task-specific goal state and task-specific reward term. In contrast, our framework supports fully automated goal state design and switching, as well as a unified reward signal.

Goal state via RMD. At time step t , given the i -th plan interaction step $\mathcal{G}_i = \{\mathcal{T}_H, \mathcal{B}, \mathcal{T}_O\}$, we first encode each edge e_{ij} from \mathcal{B} by collecting the corresponding absolute position $\mathbf{p}_{h_i}^p$ and absolute velocity $\mathbf{p}_{h_i}^v$ of the human part joint \mathbf{p}_{h_i} , as well as the absolute position $\mathbf{p}_{o_j}^p$ and absolute velocity $\mathbf{p}_{o_j}^v$ of the nearest point in the object part point cloud $\mathbf{p}_{o_j} \in \mathbb{R}^3$ from the simulation environment. Next, we calculate the relative position $\tilde{\mathbf{p}}_{ij}$ and the relative velocity $\tilde{\mathbf{v}}_{ij}$ for each pair of points and transform these quantities into the agent’s coordinate system. For each edge, a one-hot encoding w'_{ij} is applied to represent w_{ij} . The one-hot vector w'_{ij} is then concatenated with the regularized relative position $\tilde{\mathbf{p}}_{ij}$ and relative velocity $\tilde{\mathbf{v}}_{ij}$ at time step t , yielding the rmd state representation $\mathbf{s}_t^{\text{rmd}} = \{\tilde{\mathbf{p}}_{ij}, \tilde{\mathbf{v}}_{ij}, w'_{ij}\}$. Both \mathcal{T}_H and \mathcal{T}_O are in the form `object(spatial relationship type)`. In our implementation, we first compute the object’s bounding box and get s_x, s_y, s_z , which correspond to the size of the object along the x -, y -, or z -axis, respectively. The position is then determined by shifting from the object center to the target according to the specific spatial relationship type. For instance, `armchair(front)` represents a position that is $(0.7s_x, 0, 0)$ in the armchair’s local coordinate system. Next, we transform the positions of \mathcal{T}_H and \mathcal{T}_O into the agent’s coordinate system. This transformation guides both the agent’s and the object’s trajectories, yielding the destination state $\mathbf{d}_t = \{\mathbf{d}_t^h, \mathbf{d}_t^o\}$. To enhance the agent’s ability to perceive its surrounding local environment and avoid obstacles, a resolution-fixed height map \mathbf{h}_t is incorporated, which records the heights of nearby object geometries aligned with the root’s facing direction [35, 45]. Furthermore, to enhance object perception, key parameters are extracted: the eight vertices of the bounding box $\mathbf{b}_t^{\text{ver}}$, the rotation angle θ_t , the linear velocity \mathbf{v}_t , and the angular velocity \mathbf{w}_t . These parameters define the object’s state $\mathbf{o}_t = \{\mathbf{b}_t^{\text{ver}}, \theta_t, \mathbf{v}_t, \mathbf{w}_t\}$. Finally, combine $\mathbf{s}_t^{\text{rmd}}, \mathbf{d}_t, \mathbf{h}_t$, and \mathbf{o}_t , we obtain the complete set of goal state.

$$\mathbf{g}_t = \{\mathbf{s}_t^{\text{rmd}}, \mathbf{d}_t, \mathbf{h}_t, \mathbf{o}_t\}. \quad (7)$$

Reward via RMD. The task reward $r^G(\mathbf{s}_t, \mathbf{g}_t, \mathbf{s}_{t+1})$ is the weighted sum of the human root target reward, object root target reward, and RMD reward. When r^G exceeds the threshold θ , we switch the \mathcal{G}_i to the next goal \mathcal{G}_{i+1} .

$$r^G(\mathbf{s}_t, \mathbf{g}_t, \mathbf{s}_{t+1}) = \lambda_{\text{RMD}} \cdot r_{\text{RMD}} + \lambda_h \cdot r_h^{\text{tar}} + \lambda_o \cdot r_o^{\text{tar}}. \quad (8)$$

The human root target reward r_h^{tar} is designed to encourage the human root position $x_t^{h_{\text{root}}}$ to approach the target position $x_t^{h_{\text{target}}}$.

$$r_h^{\text{tar}} = \exp\left(-\left\|x_t^{h_{\text{root}}} - x_t^{h_{\text{target}}}\right\|^2\right). \quad (9)$$

The object root target reward r_o^{tar} is designed to encourage the object root position $x_t^{o_{\text{root}}}$ to approach the target position $x_t^{o_{\text{target}}}$.

$$r_o^{\text{tar}} = \exp\left(-\left\|x_t^{o_{\text{root}}} - x_t^{o_{\text{target}}}\right\|^2\right). \quad (10)$$

The RMD reward r_{RMD} is the weighted sum of r_{RMD}^k , which guides the relative movement dynamics between each human part and object part to faithfully follow the plan. Specifically, the value of r_{RMD}^k is determined by the edge weight w_{ij} from \mathcal{B} .

$$r_{\text{RMD}} = \sum_{k=1}^{15} \lambda_k \cdot r_{\text{RMD}}^k. \quad (11)$$

This reward function guides the relative movement dynamics between human parts and object parts to faithfully follow the plan. Specifically, the behavior of r_{RMD}^k is determined by the weight w_{ij} as follows:

- When $w_{ij} = 0$, r_{RMD} encourages the relative velocity between the two particles to approach zero, or the angle between their relative velocity and relative position to be approximately 0.5π .
- When $w_{ij} = 1$, the goal is for a small relative distance between the particles, minimizing the angle between their relative velocity and relative position.
- When $w_{ij} = 2$, the aim is to increase the relative distance between the particles while still minimizing the relative velocity angle.
- Finally, when $w_{ij} = 3$, it indicates an unstable relative movement trend, where the particles may either approach or move away from each other. In such cases, we directly set the reward to its maximum value.

To balance different reward weights λ in Eq. (8) and Eq. (11), we utilize adaptive weights proposed by [45]. See Appendix C of the supplementary for additional details.

4. Experiment

Our experiments are organized into two main sections: the first evaluates HOI skill learning in a single-task scenario (Sec. 4.1), and the second evaluates it in a long-horizon multi-task scenario (Sec. 4.2).

Methods	Completion Rate (%) \uparrow						Success Rate (%) \uparrow						Precision (cm) \downarrow					
	Carry	Push	Open	Sit	Lie	Reach	Carry	Push	Open	Sit	Lie	Reach	Carry	Push	Open	Sit	Lie	Reach
UniHSI[45]	-	-	-	58.9	23.2	97.1	-	-	-	94.3	81.5	97.5	-	-	-	5.6	12.8	2.1
AMP*[27]	53.2	40.4	63.2	7.4	0.9	93.2	74.9	71.0	70.3	77.4	51.9	92.2	17.3	31.7	18.1	13.2	19.1	5.5
InterPhys*[9]	67.8	47.1	83.2	23.2	2.7	95.3	88.2	78.1	90.1	88.1	76.4	95.9	12.3	24.7	10.1	10.3	14.8	3.4
Ours	88.3	84.1	91.2	92.6	62.0	97.5	93.3	90.1	95.1	95.6	87.0	97.8	10.1	18.2	5.2	4.9	9.1	1.9
multi-one	75.1	71.3	77.9	81.0	49.2	96.2	90.5	86.4	92.1	94.2	83.1	97.2	13.6	21.0	7.3	5.5	14.3	2.0
one-multi	11.7	59.2	68.7	65.8	28.1	97.2	14.3	81.2	90.8	92.3	81.6	97.4	21.3	32.2	7.2	9.1	17.2	2.0
w.o. $\tilde{\mathbf{p}}_{ij}$	71.7	73.8	77.0	72.9	36.8	96.8	88.9	87.8	90.3	91.8	79.8	96.8	10.9	19.7	10.1	5.6	12.8	2.9
w.o. $\tilde{\mathbf{v}}_{ij}$	78.2	76.7	75.2	76.1	42.1	96.9	90.1	84.2	87.8	92.1	79.2	96.9	11.3	20.0	9.9	6.1	14.2	2.5
w.o. w_{ij}^l	69.1	68.4	62.1	67.0	30.3	95.1	82.3	82.3	86.2	90.3	78.9	95.2	14.1	23.9	9.2	7.6	18.6	2.2

Table 2. **Comparison with Baselines in Single-Task Scenario.** * Indicates that these baselines have been re-implemented based on their original papers or publicly available code to ensure a consistent experimental setup. Our method achieves state-of-the-art quantitative results in both static and dynamic interaction tasks.

Implementation Details. To ensure our agent interacts with objects in a natural way, we collect motion clips from SAMP [9], OMOMO [14], CIRCLE [2]. We conduct experiments in parallel simulated environments within Isaac-Gym [21], using PyTorch for neural network implementation. In line with previous studies [9, 45], our physical humanoid model consists of 15 rigid body parts and 28 joints, all controlled by a PD controller. The simulator operates at a frequency of 60 Hz, while policy updates are made at 30 Hz. We utilize Proximal Policy Optimization (PPO) [29] to train the policy network on an NVIDIA RTX 3090 GPU.

4.1. Comparisons in a Single-Task Scenario

Settings. We select a set of interaction tasks that are commonly used in prior works, as well as some novel tasks that have not been previously reported. These include three static HOI tasks: reaching, sitting, and lying down, and three dynamic HOI tasks: carrying, pushing, and opening. While previous works [9, 45] primarily focus on the approach and interaction with objects, they often overlook a critical aspect: after interacting with an object, the agent must return to a neutral state to facilitate subsequent interactions. For instance, in the sitting task, previous methods consider the task complete once the agent is seated. However, this disregards the need for the agent to return to a standing position in order to transition smoothly to the next task. Therefore, we redefine the task completion criteria by introducing a “leaving” step: after interacting with an object, the agent must stand up and walk to a designated position. This step ensures that the agent returns to a neutral pose, which is essential for smooth transitions between tasks. In line with prior works, we use static, movable, and articulated objects from PartNet [23], 3D-Front [6], CIRCLE [2], SAMP [8], and PartNet-Mobility [44]. For each episode, objects are initialized with a random orientation (ranging from 0 to 2π), a random distance (from 4 to 10 meters), and a random scale (from 0.8 to 1.2). The finish

position is then randomly sampled at a point 3 meters away from the object. To ensure a fair comparison with previous state-of-the-art methods, we modify the implementations of AMP [27], InterPhys [9], and UniHSI [45] by adjusting their goal states and corresponding reward functions.

Metrics. In line with prior works [9, 45], we report the **Success Rate** to measure the percentage of trials in which the character successfully interacts with the object. A trial is considered successful if the distance between the object’s root and a specific humanoid part is less than 20 cm (for tasks like reaching, sitting, or lying down) or if the distance between the object’s root and the target location is less than 20 cm (for tasks like carrying, pushing, or opening). Additionally, we report the **Completion Rate**, which measures the percentage of trials in which the character successfully completes the interaction with the object and returns to a neutral standing pose (with the character’s root within 20 cm of the finish position). Furthermore, we utilize **Precision** to quantify the average distance between a specific human body part and its corresponding target position over the course of the entire interaction in successfully completed trials. All metrics are evaluated over 4096 trials per task.

Result Analysis. As shown in Tab. 2, our method achieves higher or comparable performance across all these metrics compared to the baselines. Our method outperforms tasks involving the recovery process of static human-object interactions, such as getting up after sitting or lying down, as the Relative Movement Dynamics guide each body part to move away from the object. In contrast, as shown in Fig. 3, UniHSI [45] struggles to get up because it treats the human-object interaction as a sequence of independent spatial reaching tasks, neglecting the temporal dynamics that coordinate the movements of different body parts. Similarly, InterPhys [9] produces unnatural and unstable motions to complete tasks, such as abrupt kicking or thrust-

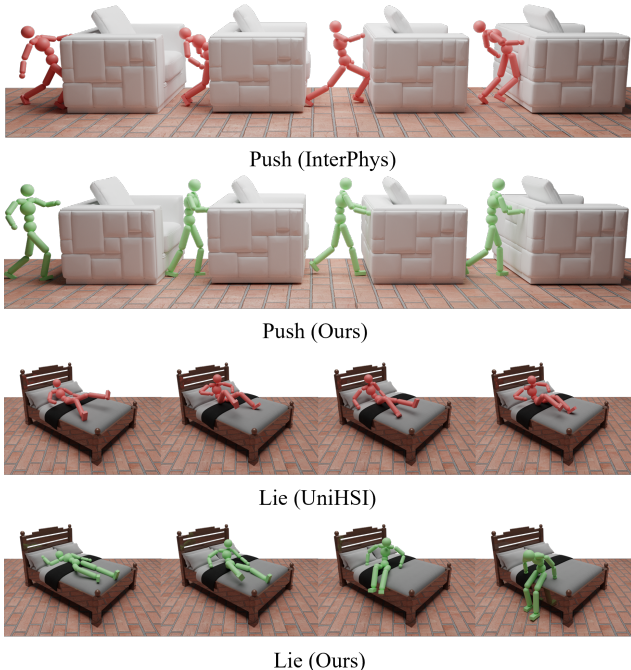


Figure 3. **Visualization for Qualitative Comparison.** Other methods exhibit unnatural motion (InterPhys) or incomplete interactions (UniHSI), whereas our method demonstrates human-like motion quality in qualitative assessments. More qualitative visualization videos can be found in the supplementary materials.

ing forward, due to its lack of fine-grained spatial-temporal guidance for coordinating the movements of different body parts. Instead, our design ensures that the agent keeps both hands and arms relatively stationary against the back of the sofa. More qualitative visualization videos can be found in the supplementary materials.

Ablation. We perform an ablation study on key components to demonstrate the impact of the proposed RMD. In the multi-one setup, we simplify the object representation by removing the division into distinct parts based on geometry and interaction types. Instead, we treat the object as a single entity. This modification leads to slight performance degradation as the model loses a finer-grained understanding of object geometry. Instead, we represent the object’s pose and kinematic information using the root pose and its kinematic data. This leads to a slight degradation in model performance, as it lacks a more fine-grained perception of object geometry. In the one-multi setup, we constrain our RMD Planner to model only the dynamics of a single human part interacting with one of the multiple object parts in each planned substep. This configuration is somewhat similar to UniHSI [45], and it results in an overall decline in performance metrics since setting a target for

only a single body part disrupts the overall coordination of human movement and is likely to cause the optimization process to become stuck in a local optimum. The results demonstrate that our multi-multi objective significantly enhances performance in complex and challenging interaction scenarios. Furthermore, removing kinematic relation encoding ($\tilde{p}_t^{ij}, \tilde{v}_t^{ij}$) or dynamic encoding (w_t^{ij}) harms performance since these components capture the spatial-temporal relationship between the human and the object during interaction. Overall, the proposed RMD plays an important role in ensuring the humanoid interacts completely with the object: approaching, interacting, and returning to an appropriate initial state.

4.2. Comparisons in a Multi-Task Scenario

While the single-task experiments provide valuable insights into the agent’s performance in handling individual human-object interactions, they focus on isolated tasks. However, real-world applications require the agent to manage multiple tasks either concurrently or sequentially, demanding more sophisticated coordination and planning. To evaluate the robustness of our method in such complex settings, we extend our experiments to a multi-task scenario. In this setup, the agent must handle various tasks within a single plan, which challenges the scalability and adaptability of the proposed Relative Movement Dynamics framework. This extension tests the ability of RMD to manage long-horizon, multi-task interactions. To support training and evaluation in this context, we introduce a new dataset, InterPlay, which contains thousands of interaction plans involving static, dynamic, and articulated objects.

InterPlay Dataset. We utilize high-quality 3D object assets from existing datasets, including PartNet [23], 3D-FRONT [6], SAMP [8], CIRCLE [2], and PartNet-Mobility [44]. These datasets offer a diverse and detailed collection of 3D models that form the backbone of our experimental framework. We manually verified and further annotated the parts and corresponding point clouds of these 3D assets to ensure data consistency and high fidelity. During both training and inference, we randomly sampled at least two objects for interaction, while optionally including additional objects to provide a more comprehensive scene context. For each object, we randomly assigned its size, initial position, and rotation, thereby generating a wide range of spatial layouts that mimic real-world variability. We then rendered top-view images of the layout context and employed our RMD Planner to generate detailed, context-aware plans based on the given instructions. In total, we generated 1,210 plans, encompassing a wide variety of human-object interactions—including static, dynamic, and articulated objects—with varying temporal horizons within an indoor layout.

Methods	Completion Rate (%) \uparrow			Sub-step Completion Ratio (%) \uparrow			Sub-step Precision (cm) \downarrow		
	Static Interaction	Dynamic Interaction	Hybrid	Static Interaction	Dynamic Interaction	Hybrid	Static Interaction	Dynamic Interaction	Hybrid
UniHSI[45]	31.2	-	-	61.3	-	-	10.2	-	-
InterPhys*[9]	11.4	47.8	27.5	37.3	61.9	54.1	13.8	18.7	16.9
Ours	75.1	71.2	53.8	86.2	84.3	71.8	7.7	13.0	11.2
RMD-LLM	62.8	53.1	39.9	81.7	78.3	67.2	8.9	15.2	13.8

Table 3. **Comparison with Baselines in Long-Horizon Multi-Task Scenarios.** * Indicates the use of a vanilla combination and switching of different task policies, as the original InterPhys framework cannot handle multi-task scenarios.

Settings. We split our dataset into three categories: static-interaction, dynamic-interaction, and hybrid setups. In the static-only setup, we sequentially interact with at least two static objects as planned in the dataset. In the dynamic-only setup, we sequentially interact with at least two dynamic objects or articulated objects, also following the pre-planned dataset structure. In the hybrid setup, we select at least three objects, ensuring that at least one dynamic human-object interaction task is included in the overall plan. Since UniHSI [45] supports only sequential interactions with static objects, we adapt their released prompt to generate plans based on scenarios from our InterPlay-static-only dataset. InterPhys [9] supports both dynamic and static interaction tasks, but it is a task-specific policy. For a fair comparison, we combine multiple tasks in a vanilla setup to train a multi-task policy. We use one-hot encoding to represent different tasks and switch to the next goal based on heuristic rules.

Metrics. Following Sec. 4.1, we report the **Completion Rate**, which measures the percentage of trials in which the character can sequentially complete all sub-step tasks and return to a natural standing pose, with the character’s root within 20 cm of the target position. We introduce the **Sub-step Completion Ratio**, which measures the ratio of completed sub-steps to the total number of planned sub-steps. This metric provides a more granular view of the agent’s ability to handle complex tasks with multiple sub-goals. Additionally, we use **Sub-step Precision** to measure the average distance between a specific human part and its corresponding target position, or between the object root and its corresponding target position.

Result Analysis. Our method benefits from a unified formulation of interaction and fine-grained spatial-temporal guidance for all human body parts, enabling seamless transitions to a multi-task setup. This design not only streamlines the training process by maintaining consistent representations across various tasks but also significantly improves the model’s ability to generalize across different interaction scenarios. The approach achieves state-of-the-art performance in both individual sub-step execution and

long-horizon transitions, reflecting its robustness in handling intricate sequences of actions. Without such a unified formulation, the straightforward combination of different tasks [9] often leads to interference between task-specific features and inefficient training dynamics. In contrast, our integrated method preserves critical spatial and temporal information throughout the pipeline. While UniHSI [45] excels at approaching and interacting with static objects, it struggles with actions such as getting up after interaction, which notably limits its performance in long-horizon scenarios. More qualitative visualization videos can be found in the supplementary materials.

Ablation. While both VLMs and LLMs have extensive world knowledge, VLMs offer more precise spatial awareness owing to their seamless integration of visual and textual data. To explore this further, we modified the input data by replacing top-view images with richly descriptive paragraphs that detail the objects in the scene, outline their various parts, and specify their relative spatial positions. This modification allowed us to rigorously evaluate the performance of a LLM-based planner under conditions lacking explicit visual cues. The results clearly indicate that the spatial perception capability inherent in the vision model plays a critical role in facilitating effective planning.

5. Conclusion

In this paper, we proposed a unified framework for Human-Object Interaction (HOI) that leverages the concept of Relative Movement Dynamics (RMD) to model complex spatial-temporal interactions between humans and objects. By integrating vision-language models (VLMs) for high-level planning and goal-conditioned reinforcement learning for precise task execution, our approach enables long-term, physically plausible interactions. We also introduced InterPlay, a diverse dataset designed to support training and evaluation across a wide range of static and dynamic HOI tasks. Extensive experiments demonstrate that our framework outperforms state-of-the-art methods in both single-task and multi-task scenarios, achieving higher task completion rates and greater interaction precision.

6. Acknowledgement

This work was supported by Shanghai Local College Capacity Building Program (23010503100), National Natural Science Foundation of China (No.62406195), MoE Key Laboratory of Intelligent Perception and Human-Machine Collaboration, HPC Platform of ShanghaiTech University and Shanghai Engineering Research Center of Intelligent Vision and Imaging.

References

- [1] Josh Achiam, Steven Adler, Sandhini Agarwal, Lama Ahmad, Ilge Akkaya, Florencia Leoni Aleman, Diogo Almeida, Janko Altenschmidt, Sam Altman, Shyamal Anadkat, et al. Gpt-4 technical report. *arXiv preprint arXiv:2303.08774*, 2023. 4
- [2] Joao Pedro Araújo, Jiaman Li, Karthik Vetrivel, Rishi Agarwal, Jiajun Wu, Deepak Gopinath, Alexander William Clegg, and Karen Liu. Circle: Capture in rich contextual environments. In *Proceedings of the IEEE/CVF Conference on Computer Vision and Pattern Recognition*, pages 21211–21221, 2023. 6, 7
- [3] Yu-Wei Chao, Jimei Yang, Weifeng Chen, and Jia Deng. Learning to sit: Synthesizing human-chair interactions via hierarchical control. In *Proceedings of the AAAI Conference on Artificial Intelligence*, pages 5887–5895, 2021. 2, 3
- [4] Matt Deitke, Eli VanderBilt, Alvaro Herrasti, Luca Weihs, Kiana Ehsani, Jordi Salvador, Winson Han, Eric Kolve, Aniruddha Kembhavi, and Roozbeh Mottaghi. Proctor: Large-scale embodied ai using procedural generation. *Advances in Neural Information Processing Systems*, 35:5982–5994, 2022. 2
- [5] Christian Diller and Angela Dai. Cg-hoi: Contact-guided 3d human-object interaction generation. In *Proceedings of the IEEE/CVF Conference on Computer Vision and Pattern Recognition*, pages 19888–19901, 2024. 3
- [6] Huan Fu, Bowen Cai, Lin Gao, Ling-Xiao Zhang, Jiaming Wang, Cao Li, Qixun Zeng, Chengyue Sun, Rongfei Jia, Bin-qiang Zhao, et al. 3d-front: 3d furnished rooms with layouts and semantics. In *Proceedings of the IEEE/CVF International Conference on Computer Vision*, pages 10933–10942, 2021. 6, 7
- [7] Jiawei Gao, Ziqin Wang, Zeqi Xiao, Jingbo Wang, Tai Wang, Jinkun Cao, Xiaolin Hu, Si Liu, Jifeng Dai, and Jiangmiao Pang. Coohei: Learning cooperative human-object interaction with manipulated object dynamics. *arXiv preprint arXiv:2406.14558*, 2024. 2
- [8] Mohamed Hassan, Duygu Ceylan, Ruben Villegas, Jun Saito, Jimei Yang, Yi Zhou, and Michael J Black. Stochastic scene-aware motion prediction. In *Proceedings of the IEEE/CVF International Conference on Computer Vision*, pages 11374–11384, 2021. 2, 3, 6, 7
- [9] Mohamed Hassan, Yunrong Guo, Tingwu Wang, Michael Black, Sanja Fidler, and Xue Bin Peng. Synthesizing physical character-scene interactions. In *ACM SIGGRAPH 2023 Conference Proceedings*, pages 1–9, 2023. 2, 3, 6, 8, 12
- [10] Jonathan Ho, Ajay Jain, and Pieter Abbeel. Denoising diffusion probabilistic models. *Advances in neural information processing systems*, 33:6840–6851, 2020. 3
- [11] Siyuan Huang, Zan Wang, Puhao Li, Baoxiong Jia, Tengyu Liu, Yixin Zhu, Wei Liang, and Song-Chun Zhu. Diffusion-based generation, optimization, and planning in 3d scenes. In *Proceedings of the IEEE/CVF Conference on Computer Vision and Pattern Recognition*, pages 16750–16761, 2023. 2, 3
- [12] Nan Jiang, Tengyu Liu, Zhexuan Cao, Jieming Cui, Yixin Chen, He Wang, Yixin Zhu, and Siyuan Huang. Chairs: Towards full-body articulated human-object interaction. *arXiv preprint arXiv:2212.10621*, 3, 2022. 3
- [13] Nan Jiang, Zhiyuan Zhang, Hongjie Li, Xiaoxuan Ma, Zan Wang, Yixin Chen, Tengyu Liu, Yixin Zhu, and Siyuan Huang. Scaling up dynamic human-scene interaction modeling. In *Proceedings of the IEEE/CVF Conference on Computer Vision and Pattern Recognition*, pages 1737–1747, 2024. 3
- [14] Jiaman Li, Alexander Clegg, Roozbeh Mottaghi, Jiajun Wu, Xavier Puig, and C Karen Liu. Controllable human-object interaction synthesis. *arXiv preprint arXiv:2312.03913*, 2023. 2, 3, 6
- [15] Jiaman Li, Jiajun Wu, and C Karen Liu. Object motion guided human motion synthesis. *ACM Transactions on Graphics (TOG)*, 42(6):1–11, 2023. 3
- [16] Xueting Li, Sifei Liu, Kihwan Kim, Xiaolong Wang, Ming-Hsuan Yang, and Jan Kautz. Putting humans in a scene: Learning affordance in 3d indoor environments. In *Proceedings of the IEEE/CVF conference on computer vision and pattern recognition*, pages 12368–12376, 2019. 2
- [17] Libin Liu and Jessica Hodgins. Learning to schedule control fragments for physics-based characters using deep q-learning. *ACM Transactions on Graphics (TOG)*, 36(3):1–14, 2017. 4
- [18] Siqi Liu, Guy Lever, Zhe Wang, Josh Merel, SM Ali Eslami, Daniel Hennes, Wojciech M Czarnecki, Yuval Tassa, Shayegan Omidshafiei, Abbas Abdolmaleki, et al. From motor control to team play in simulated humanoid football. *Science Robotics*, 7(69):eabo0235, 2022. 4
- [19] Zhengyi Luo, Jiashun Wang, Kangni Liu, Haotian Zhang, Chen Tessler, Jingbo Wang, Ye Yuan, Jinkun Cao, Zihui Lin, Fengyi Wang, et al. Smpolympics: Sports environments for physically simulated humanoids. *arXiv preprint arXiv:2407.00187*, 2024. 4
- [20] Yecheng Jason Ma, William Liang, Guanzhi Wang, De-An Huang, Osbert Bastani, Dinesh Jayaraman, Yuke Zhu, Linxi Fan, and Anima Anandkumar. Eureka: Human-level reward design via coding large language models. *arXiv preprint arXiv: Arxiv-2310.12931*, 2023. 2
- [21] Viktor Makoviychuk, Lukasz Wawrzyniak, Yunrong Guo, Michelle Lu, Kier Storey, Miles Macklin, David Hoeller, Nikita Rudin, Arthur Allshire, Ankur Handa, et al. Isaac gym: High performance gpu-based physics simulation for robot learning. *arXiv preprint arXiv:2108.10470*, 2021. 2, 6
- [22] Josh Merel, Saran Tunyasuvunakool, Arun Ahuja, Yuval Tassa, Leonard Hasenclever, Vu Pham, Tom Erez, Greg

- Wayne, and Nicolas Heess. Catch & carry: reusable neural controllers for vision-guided whole-body tasks. *ACM Transactions on Graphics (TOG)*, 39(4):39–1, 2020. 3
- [23] Kaichun Mo, Shilin Zhu, Angel X. Chang, Li Yi, Subarna Tripathi, Leonidas J. Guibas, and Hao Su. PartNet: A large-scale benchmark for fine-grained and hierarchical part-level 3D object understanding. In *The IEEE Conference on Computer Vision and Pattern Recognition (CVPR)*, 2019. 6, 7
- [24] Damian Mrowca, Chengxu Zhuang, Elias Wang, Nick Haber, Li F Fei-Fei, Josh Tenenbaum, and Daniel L Yamins. Flexible neural representation for physics prediction. *Advances in neural information processing systems*, 31, 2018. 1
- [25] Xiaogang Peng, Yiming Xie, Zizhao Wu, Varun Jampani, Deqing Sun, and Huaizu Jiang. Hoi-diff: Text-driven synthesis of 3d human-object interactions using diffusion models. *arXiv preprint arXiv:2312.06553*, 2023. 3
- [26] Xue Bin Peng, Pieter Abbeel, Sergey Levine, and Michiel Van de Panne. Deepmimic: Example-guided deep reinforcement learning of physics-based character skills. *ACM Transactions On Graphics (TOG)*, 37(4):1–14, 2018. 3
- [27] Xue Bin Peng, Ze Ma, Pieter Abbeel, Sergey Levine, and Angjoo Kanazawa. Amp: Adversarial motion priors for stylized physics-based character control. *ACM Transactions on Graphics (ToG)*, 40(4):1–20, 2021. 2, 3, 5, 6
- [28] Huaijin Pi, Sida Peng, Minghui Yang, Xiaowei Zhou, and Hujun Bao. Hierarchical generation of human-object interactions with diffusion probabilistic models. In *Proceedings of the IEEE/CVF International Conference on Computer Vision*, pages 15061–15073, 2023. 3
- [29] John Schulman, Filip Wolski, Prafulla Dhariwal, Alec Radford, and Oleg Klimov. Proximal policy optimization algorithms. *arXiv preprint arXiv:1707.06347*, 2017. 6
- [30] Sebastian Starke, He Zhang, Taku Komura, and Jun Saito. Neural state machine for character-scene interactions. *ACM Transactions on Graphics*, 38(6):178, 2019. 2
- [31] Sebastian Starke, Yiwei Zhao, Taku Komura, and Kazi Zaman. Local motion phases for learning multi-contact character movements. *ACM Transactions on Graphics (TOG)*, 39(4):54–1, 2020. 3
- [32] Richard S. Sutton and Andrew G. Barto. *Reinforcement Learning: An Introduction*. A Bradford Book, Cambridge, MA, USA, 2018. 2
- [33] Andrew Szot, Alexander Clegg, Eric Undersander, Erik Wijmans, Yili Zhao, John Turner, Noah Maestre, Mustafa Mukadam, Devendra Singh Chaplot, Oleksandr Maksymets, et al. Habitat 2.0: Training home assistants to rearrange their habitat. *Advances in neural information processing systems*, 34:251–266, 2021. 2
- [34] Jiangnan Tang, Jingya Wang, Kaiyang Ji, Lan Xu, Jingyi Yu, and Ye Shi. A unified diffusion framework for scene-aware human motion estimation from sparse signals. In *Proceedings of the IEEE/CVF Conference on Computer Vision and Pattern Recognition*, pages 21251–21262, 2024. 3
- [35] Chen Tessler, Yunrong Guo, Ofir Nabati, Gal Chechik, and Xue Bin Peng. Maskedmimic: Unified physics-based character control through masked motion inpainting. *ACM Transactions on Graphics (TOG)*, 2024. 5
- [36] Guy Tevet, Sigal Raab, Setareh Cohan, Daniele Reda, Zhengyi Luo, Xue Bin Peng, Amit H Bermano, and Michiel van de Panne. Clo3d: Closing the loop between simulation and diffusion for multi-task character control. *arXiv preprint arXiv:2410.03441*, 2024. 3
- [37] Emanuel Todorov, Tom Erez, and Yuval Tassa. Mujoco: A physics engine for model-based control. In *2012 IEEE/RSJ international conference on intelligent robots and systems*, pages 5026–5033. IEEE, 2012. 2
- [38] Jiashun Wang, Huazhe Xu, Jingwei Xu, Sifei Liu, and Xiaolong Wang. Synthesizing long-term 3d human motion and interaction in 3d scenes, 2020. 3
- [39] Jingbo Wang, Yu Rong, Jingyuan Liu, Sijie Yan, Dahua Lin, and Bo Dai. Towards diverse and natural scene-aware 3d human motion synthesis. In *Proceedings of the IEEE/CVF Conference on Computer Vision and Pattern Recognition*, pages 20460–20469, 2022. 3
- [40] Yinhuai Wang, Jing Lin, Ailing Zeng, Zhengyi Luo, Jian Zhang, and Lei Zhang. Physshoi: Physics-based imitation of dynamic human-object interaction. *arXiv preprint arXiv:2312.04393*, 2023. 2, 4
- [41] Yinhuai Wang, Qihan Zhao, Runyi Yu, Ailing Zeng, Jing Lin, Zhengyi Luo, Hok Wai Tsui, Jiwen Yu, Xiu Li, Qifeng Chen, et al. Skillmimic: Learning reusable basketball skills from demonstrations. *arXiv preprint arXiv:2408.15270*, 2024. 2, 4
- [42] Qianyang Wu, Ye Shi, Xiaoshui Huang, Jingyi Yu, Lan Xu, and Jingya Wang. Thor: Text to human-object interaction diffusion via relation intervention. *arXiv preprint arXiv:2403.11208*, 2024. 3
- [43] Zhen Wu, Jiaman Li, Pei Xu, and C. Karen Liu. Human-object interaction from human-level instructions, 2024. 3
- [44] Fanbo Xiang, Yuzhe Qin, Kaichun Mo, Yikuan Xia, Hao Zhu, Fangchen Liu, Minghua Liu, Hanxiao Jiang, Yifu Yuan, He Wang, Li Yi, Angel X. Chang, Leonidas J. Guibas, and Hao Su. SAPIEN: A simulated part-based interactive environment. In *The IEEE Conference on Computer Vision and Pattern Recognition (CVPR)*, 2020. 6, 7
- [45] Zeqi Xiao, Tai Wang, Jingbo Wang, Jinkun Cao, Wenwei Zhang, Bo Dai, Dahua Lin, and Jiangmiao Pang. Unified human-scene interaction via prompted chain-of-contacts. In *The Twelfth International Conference on Learning Representations*, 2024. 2, 3, 5, 6, 7, 8, 12
- [46] Zhaoming Xie, Sebastian Starke, Hung Yu Ling, and Michiel van de Panne. Learning soccer juggling skills with layer-wise mixture-of-experts. In *ACM SIGGRAPH 2022 Conference Proceedings*, pages 1–9, 2022. 4
- [47] Zhaoming Xie, Jonathan Tseng, Sebastian Starke, Michiel van de Panne, and C Karen Liu. Hierarchical planning and control for box loco-manipulation. *Proceedings of the ACM on Computer Graphics and Interactive Techniques*, 6(3):1–18, 2023. 3
- [48] Sirui Xu, Ziyin Wang, Yu-Xiong Wang, and Liang-Yan Gui. Interdreamer: Zero-shot text to 3d dynamic human-object interaction. *arXiv preprint arXiv:2403.19652*, 2024. 3
- [49] Sirui Xu, Hung Yu Ling, Yu-Xiong Wang, and Liangyan Gui. Intermimic: Towards universal whole-body control for physics-based human-object interactions. In *CVPR*, 2025. 3

- [50] Xinyu Xu, Yizheng Zhang, Yong-Lu Li, Lei Han, and Cewu Lu. Humanvla: Towards vision-language directed object rearrangement by physical humanoid. *arXiv preprint arXiv:2406.19972*, 2024. 2
- [51] Haibiao Xuan, Xiongzhen Li, Jinsong Zhang, Hongwen Zhang, Yebin Liu, and Kun Li. Narrator: Towards natural control of human-scene interaction generation via relationship reasoning. In *Proceedings of the IEEE/CVF International Conference on Computer Vision (ICCV)*, pages 22268–22278, 2023. 2
- [52] Hongwei Yi, Justus Thies, Michael J Black, Xue Bin Peng, and Davis Rempe. Generating human interaction motions in scenes with text control. In *European Conference on Computer Vision*, pages 246–263. Springer, 2025. 3
- [53] Herman Zanstra. A study of relative motion in connection with classical mechanics. *Physical Review*, 23(4):528, 1924. 2
- [54] Chengwen Zhang, Yun Liu, Ruofan Xing, Bingda Tang, and Li Yi. Core4d: A 4d human-object-human interaction dataset for collaborative object rearrangement. *arXiv preprint arXiv:2406.19353*, 2024. 3
- [55] Haotian Zhang, Ye Yuan, Viktor Makovychuk, Yunrong Guo, Sanja Fidler, Xue Bin Peng, and Kayvon Fatahalian. Learning physically simulated tennis skills from broadcast videos. *ACM Transactions on Graphics (TOG)*, 42(4):1–14, 2023. 4
- [56] Siwei Zhang, Yan Zhang, Qianli Ma, Michael J Black, and Siyu Tang. Generating person-scene interactions in 3d scenes. In *International Conference on 3D Vision (3DV)*, 2020. 2
- [57] Xiaohan Zhang, Bharat Lal Bhatnagar, Sebastian Starke, Vladimir Guzov, and Gerard Pons-Moll. Couch: Towards controllable human-chair interactions. In *European Conference on Computer Vision*, pages 518–535. Springer, 2022. 2, 3
- [58] Yan Zhang and Siyu Tang. The wanderings of odysseus in 3d scenes. In *Proceedings of the IEEE/CVF Conference on Computer Vision and Pattern Recognition*, pages 20481–20491, 2022. 3
- [59] Kaifeng Zhao, Shaofei Wang, Yan Zhang, Thabo Beeler, and Siyu Tang. Compositional human-scene interaction synthesis with semantic control. In *European conference on computer vision (ECCV)*, 2022. 2
- [60] Kaifeng Zhao, Yan Zhang, Shaofei Wang, Thabo Beeler, and Siyu Tang. Synthesizing diverse human motions in 3d indoor scenes. In *Proceedings of the IEEE/CVF International Conference on Computer Vision*, pages 14738–14749, 2023. 3
- [61] Kaifeng Zhao, Gen Li, and Siyu Tang. Dart: A diffusion-based autoregressive motion model for real-time text-driven motion control. *arXiv preprint arXiv:2410.05260*, 2024. 3
- [62] Juntian Zheng, Qingyuan Zheng, Lixing Fang, Yun Liu, and Li Yi. Cams: Canonicalized manipulation spaces for category-level functional hand-object manipulation synthesis. In *Proceedings of the IEEE/CVF Conference on Computer Vision and Pattern Recognition*, pages 585–594, 2023. 1
- [63] Keyang Zhou, Bharat Lal Bhatnagar, Jan Eric Lenssen, and Gerard Pons-Moll. Toch: Spatio-temporal object-to-hand correspondence for motion refinement. In *European Conference on Computer Vision*, pages 1–19. Springer, 2022.
- [64] Guangxiang Zhu, Zhiao Huang, and Chongjie Zhang. Object-oriented dynamics predictor. *Advances in Neural Information Processing Systems*, 31, 2018. 1

Human-Object Interaction with Vision-Language Model

Guided Relative Movement Dynamics

Supplementary Material

A. Demo Video

To complement the qualitative results discussed in the main paper, we provide several demonstration videos that offer detailed visualizations of our method. These videos not only serve to illustrate the qualitative comparisons with competing approaches but also reinforce the effectiveness of our framework across various real-world scenarios. For a comprehensive understanding, we encourage the reader to refer to the supplementary materials accompanying this paper.

Single Task Scenario. Demo4.mp4 and Demo5.mp4 present a qualitative comparison between our method and UniHSI [45] for the sitting task. In these videos, when the agent attempts to stand up from a seated position, we observe that the method employed by UniHSI relies excessively on high-frequency jitter to twist the pelvis. This excessive reliance causes the agent to become stuck in a local minimum of the goal-reaching objective, leading to unrealistic and jerky motion that deviates from natural human behavior. In contrast, our method generates smooth, human-like motion, ensuring a natural transition from sitting to standing and more faithfully replicating realistic human behavior.

Additionally, Demo6.mp4 and Demo7.mp4 compare our approach with InterPhys [9] in the door-opening task. Although InterPhys achieves strong quantitative results, its generated motion appears unrealistic. Specifically, during the door-opening task, InterPhys uses only its body to push the door open, resulting in an unnatural movement pattern. In contrast, our method employs a coordinated use of both hands, which produces a more lifelike interaction and aligns closely with typical human behavior observed in similar scenarios.

Multi Task Scenario. Demo1.mp4, Demo2.mp4, and Demo3.mp4 further demonstrate long-horizon interactions involving static, dynamic, and articulated objects within a realistic indoor furniture setting. These videos illustrate how our method robustly handles multi-task scenarios by leveraging three key strengths of our framework:

1. **Human-like Motion:** Our approach is designed to ensure that the agent avoids undesirable states while transitioning smoothly between tasks. This results in fluid and coherent motions that are consistent with natural human biomechanics.
2. **Unified Objective Design:** By employing a consistent objective design across various interaction types, our framework effectively simplifies the task of multi-task

learning. This unified approach reduces the need for extensive tuning of separate objectives for different tasks.

3. **Vision-Language Model Capabilities:** The integrated Vision-Language Model (VLM) leverages its visual understanding of the spatial layout along with rich world knowledge to generate plausible and contextually relevant action plans. This capability is crucial for adapting to complex environments and ensuring realistic task execution.

B. Details of RMD Planner

As shown in Fig. 4, receiving the top-view image of the surrounding scene context and the text instruction, the RMD Planner outputs sequential sub-step plans in the form of structured JSON form so that the output can be processed directly using python script. To ensure the RMD Planner can work as we expect, we utilize different sections of prompt while each section supports individual functions. The detailed prompt for each section is listed below:

Scene-context Understanding. Figure 5 provides the detailed prompt which guides the planner. Note that we simplify the spatial relationships between objects into seven types: center, forward, back, left, right, up, and down, such relative orientation is defined according to the sub-coordinate system of the reference object.

RMD Concept Definition. In Fig. 6, we introduce the concept of Relative Movement Dynamics, represented as a bipartite graph modeling interactions between human body parts and object parts over time. The graph includes nodes for human and object parts, with edges capturing relative movement trends, such as stationary, approaching, receding, or unstable dynamics.

Specific Plan Instance. Figure 7 illustrates an instance of the output plan, demonstrating the Relative Movement Dynamics during a scenario where a humanoid bends down to grab a box with both hands. The graph details specific relationships and movement trends between body parts and object parts, showcasing the concept in action. Besides, it also plans the target position of the humanoid root and the target position of the object root.

Idea Outline. Fig. 8 provides an overview of our approach, highlighting the expected input and output of the interaction planner. Human-object interaction tasks are broken into sub-sequences, each characterized by consistent movement dynamics until transitioning to the next stage.

Plan Rules. Figure 9 outlines the rules that the planner must follow, underscoring their importance in prompt engi-

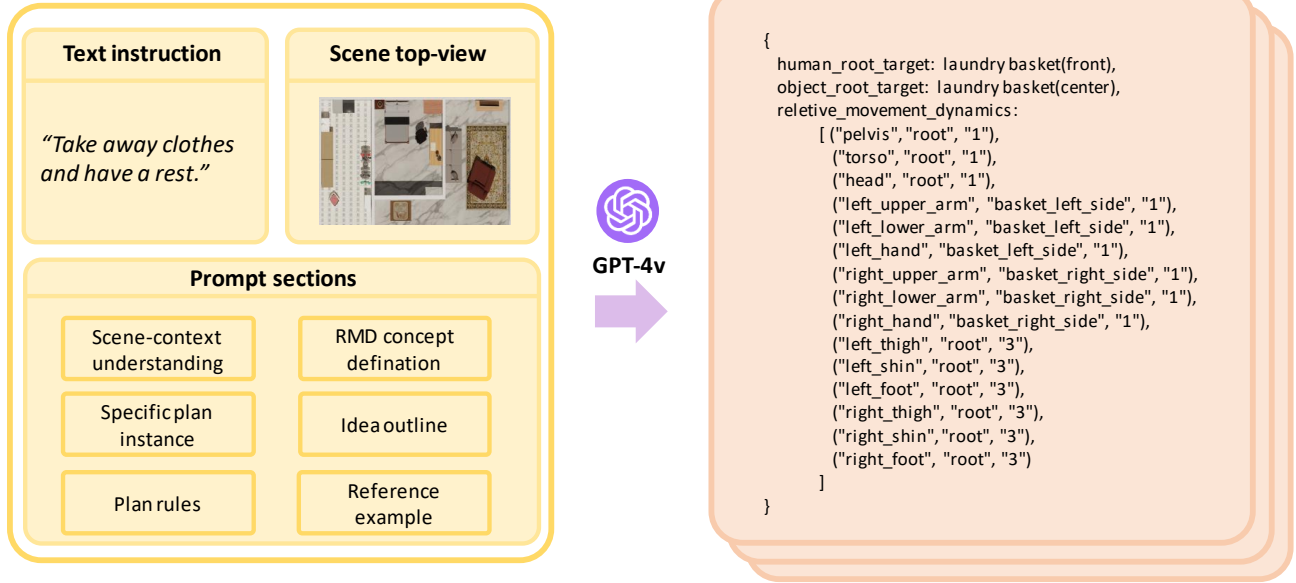


Figure 4. An overview of RMD Planner pipeline.

Prompt section1: scene-context understanding

To effectively plan sequential interactions between humanoid and objects within a scene, it is essential to recognize the type of each object, understand the spatial relationships among them, and identify the most suitable object for interaction at each sub-step, based on the scene’s top-down view. We simplify the spatial relationships between objects into seven types: center, forward, back, left, right, up, and down. For example, you can use the term "box (front)" to describe the position that lies in front of the box.

Figure 5. Details of prompt section 1.

neering. These rules ensure that the planner generates accurate and coherent sub-sequences by providing clear guidelines on task interactions, sequence formatting, and criteria for determining movement dynamics. By adhering to these rules, the planner effectively breaks down complex interactions into manageable steps, enhancing the quality and reliability of the generated plans.

Reference Example. Figures 10 to 12 sequentially presents a complete example of both input and output, clearly illustrating the concept and workflow of the planner.

C. Additional Details of Reinforcement Learning

Our physics-based animation framework is built upon goal-conditioned reinforcement learning. At each time step t , the

agent samples an action from its policy $\pi(a_t | s_t, g_t)$ based on the current state s_t and the goal state g_t . After executing the action, the environment transitions to the next state s_{t+1} , and the agent receives a task reward $r^G(s_t, g_t, s_{t+1})$. Further details on the definitions of state, reward, as well as the training procedure, are provided below.

State Definition. The state is divided into two components: the proprioception of the humanoid and object, and the goal condition. The proprioception component forms a 276-dimensional vector, encompassing the position, rotation, velocity, and angular velocity of the humanoid joints, as well as the bounding box of the object. While the root height is measured in the global reference frame, all other components are defined relative to the local frame of the character. The goal condition includes a 9×9 ego-centric heightmap, the target positions of the humanoid and object, kinematic relation encoding, and dynamic encoding for each part, resulting in a 222-dimensional vector.

Reward Definition. Recall the RMD reward r_{RMD} at time step t is the weighted sum of all the parts.

$$r_{RMD} = \sum_{k=1}^{15} w_k \cdot r_{RMD}^k. \quad (12)$$

The RMD reward for the k -th part r_{RMD}^k is defined as:

$$r_{RMD}^k = \begin{cases} r_{rv}^{still}, & \text{if } v_{ij} = 0 \\ w_{pos} \cdot r_{rp}^{close} + w_{vel} \cdot r_{rv}^{close}, & \text{if } v_{ij} = 1 \\ w_{pos} \cdot r_{rp}^{away} + w_{vel} \cdot r_{rv}^{away}, & \text{if } v_{ij} = 2 \\ 1, & \text{if } v_{ij} = 3 \end{cases} \quad (13)$$

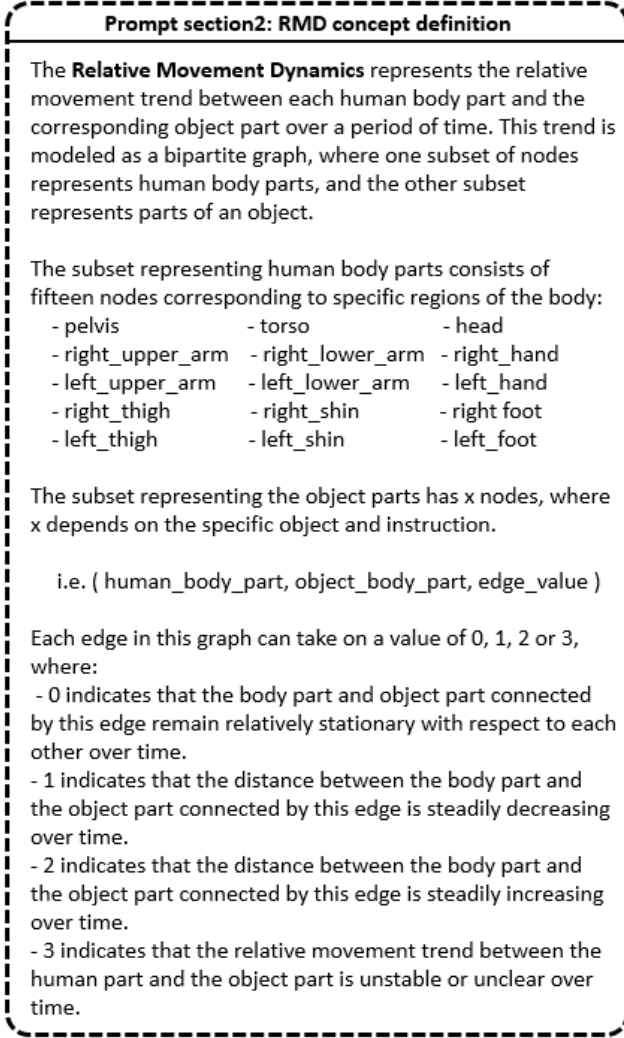


Figure 6. Details of prompt section 2.

The term r_{rv}^{still} is defined by minimizing the dot product between the relative position and relative velocity of two particles. This term encourages either the relative velocity between the two particles to approach zero or the angle between their relative velocity and relative position to approach $\frac{\pi}{2}$.

$$r_{rv}^{still} = \exp\left(-\left\|\tilde{\mathbf{p}}_t^{ij} \cdot \tilde{\mathbf{v}}_t^{ij}\right\|_2\right) \quad (14)$$

The term r_{rp}^{close} is defined to minimize the ℓ_2 norm of the relative position between the two particles, thereby encouraging them to move closer.

$$r_{rp}^{close} = \exp\left(-\left\|\tilde{\mathbf{p}}_t^{ij}\right\|_2\right) \quad (15)$$

The term r_{rv}^{close} encourages the projection of the relative velocity onto the direction of the relative position to approach a threshold. Note that the directions of these vectors are

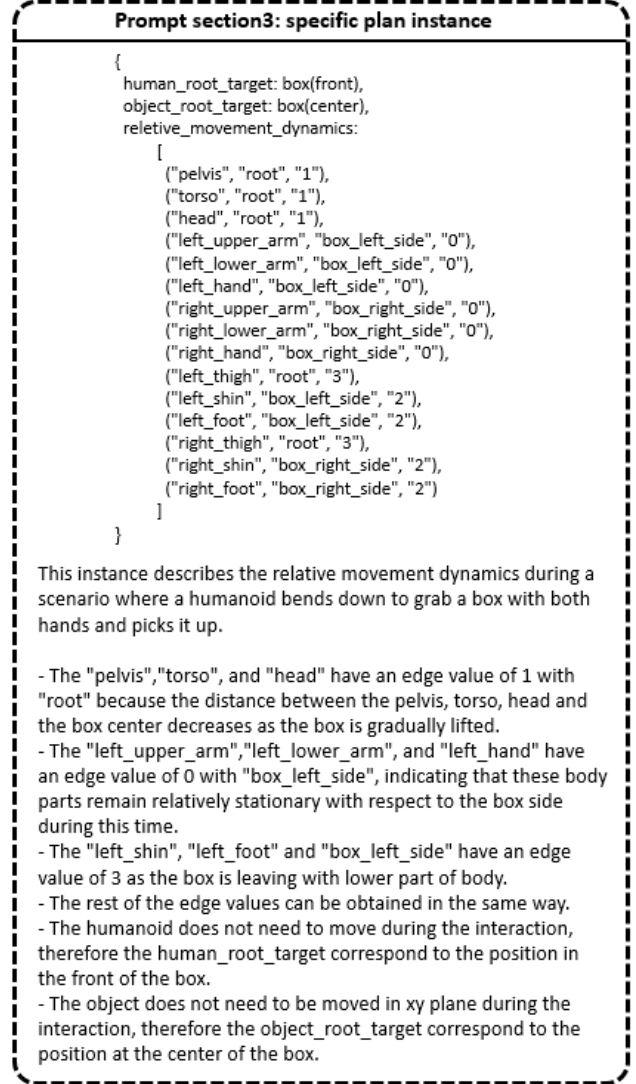


Figure 7. Details of prompt section 3.

always opposite.

$$r_{rv}^{close} = \exp\left(-\left\|\tilde{\mathbf{v}}_t^{ij} \cdot \frac{\tilde{\mathbf{p}}_t^{ij}}{\left\|\tilde{\mathbf{p}}_t^{ij}\right\|_2} + \epsilon\right\|_2\right) \quad (16)$$

The term r_{rp}^{away} is defined to maximize the ℓ_2 norm of the relative position between the two particles, promoting a greater separation between them.

$$r_{rp}^{away} = 1 - \exp\left(-\left\|\tilde{\mathbf{p}}_t^{ij}\right\|_2\right) \quad (17)$$

The term r_{rv}^{away} encourages the projection of the relative velocity onto the direction of the relative position to approach a threshold. Here, the directions of these vectors are always

Prompt section4: idea outline

Complex human-object interaction (HOI) tasks can be decomposed into several sub-sequences, where each human part maintains a consistent relative movement trend with its corresponding object part until the transition to the next sub-sequence. Therefore, we universally define the objective of the interaction plan as \mathcal{D} , with the formulation as

$$\mathcal{D} = \{\mathcal{G}_0, \mathcal{G}_1, \dots, \mathcal{G}_m\}$$

where \mathcal{G}_i denotes the i -th plan interaction step.

I will provide you with an instruction and a top-view image depicting the surrounding scene context. Your task is to break down the instruction into sub-sequences represented as relative movement dynamics, based on the top-view image. Please note that for different Human-Object Interaction (HOI) tasks, the granularity of an object's part decomposition may vary. This granularity is determined by the scene context and the instruction itself.

Figure 8. Details of prompt section 4.

Prompt section5: plan rules

1. All instructions pertain to the interaction task between a humanoid robot, modeled with relative simplicity and equipped with a ball rather than a finger on its hand, and an object. This interaction may be dynamic or static.
2. Each plan may involve sequential interactions with multiple objects. For each object, you should design a plan comprising at least five steps, including approaching and departing from the object.
3. Your return about relative_movement_dynamics should be formatted into sequence of [(human_body_part, object_body_part, edge_value), (human_body_part, object_body_part, edge_value), ...], 15 edges for one sequence.
4. If you are confused about which part of the object you should select, you can select the root to represent the whole.
5. Be relatively sensitive to the judgment of relative movement dynamics, if it is not stable (e.g. when holding a box and walking towards target, the feet and the box will alternately approach and move away from each other for a period of time), just set the value 3.

Figure 9. Details of prompt section 5.

Prompt section6: reference example-input

Instruction: Take away clothes and have a rest.

Top-view image:



Figure 10. Details of prompt section 6.

Prompt section6: reference example-output

```
step1: get close to the laundry basket.
{
  human_root_target: laundry basket(front),
  object_root_target: laundry basket(center),
  relative_movement_dynamics:
  [
    ("pelvis", "root", "1"),
    ("torso", "root", "1"),
    ("head", "root", "1"),
    ("left_upper_arm", "basket_left_side", "1"),
    ("left_lower_arm", "basket_left_side", "1"),
    ("left_hand", "basket_left_side", "1"),
    ("right_upper_arm", "basket_right_side", "1"),
    ("right_lower_arm", "basket_right_side", "1"),
    ("right_hand", "basket_right_side", "1"),
    ("left_thigh", "root", "3"),
    ("left_shin", "root", "3"),
    ("left_foot", "root", "3"),
    ("right_thigh", "root", "3"),
    ("right_shin", "root", "3"),
    ("right_foot", "root", "3")
  ]
}
```

Figure 11. Details of prompt section 6.

aligned.

$$r_{rv}^{\text{away}} = \exp \left(- \left\| \tilde{\mathbf{v}}_t^{ij} \cdot \frac{\tilde{\mathbf{p}}_t^{ij}}{\|\tilde{\mathbf{p}}_t^{ij}\|} - \epsilon \right\|_2 \right) \quad (18)$$

```

Prompt section6: reference example-output
step2: bends down to grab the box with both hands and picks it up.
{
  human_root_target: laundry basket(front),
  object_root_target: laundry basket(center),
  relative_movement_dynamics:
  [
    ("pelvis", "root", "1"),
    ("torso", "root", "1"),
    ("head", "root", "1"),
    ("left_upper_arm", "basket_left_side", "0"),
    ("left_lower_arm", "basket_left_side", "0"),
    ("left_hand", "basket_left_side", "0"),
    ("right_upper_arm", "basket_right_side", "0"),
    ("right_lower_arm", "basket_right_side", "0"),
    ("right_hand", "basket_right_side", "0"),
    ("left_thigh", "root", "3"),
    ("left_shin", "basket_left_side", "2"),
    ("left_foot", "basket_left_side", "2"),
    ("right_thigh", "root", "3"),
    ("right_shin", "basket_right_side", "2"),
    ("right_foot", "basket_right_side", "2")
  ]
}

```

```

Prompt section6: reference example-output
step3: walking to the washing machine while holding the laundry basket.
{
  human_root_target: washing machine(front),
  object_root_target: washing machine(front),
  relative_movement_dynamics:
  [
    ("pelvis", "root", "0"),
    ("torso", "root", "0"),
    ("head", "root", "0"),
    ("left_upper_arm", "basket_left_side", "0"),
    ("left_lower_arm", "basket_left_side", "0"),
    ("left_hand", "basket_left_side", "0"),
    ("right_upper_arm", "basket_right_side", "0"),
    ("right_lower_arm", "basket_right_side", "0"),
    ("right_hand", "basket_right_side", "0"),
    ("left_thigh", "root", "3"),
    ("left_shin", "root", "3"),
    ("left_foot", "root", "3"),
    ("right_thigh", "root", "3"),
    ("right_shin", "root", "3"),
    ("right_foot", "root", "3")
  ]
}

```

```

Prompt section6: reference example-output
step4: put down the laundry basket.
{
  human_root_target: washing machine(front),
  object_root_target: washing machine(front),
  relative_movement_dynamics:
  [
    ("pelvis", "root", "2"),
    ("torso", "root", "2"),
    ("head", "root", "2"),
    ("left_upper_arm", "basket_left_side", "0"),
    ("left_lower_arm", "basket_left_side", "0"),
    ("left_hand", "basket_left_side", "0"),
    ("right_upper_arm", "basket_right_side", "0"),
    ("right_lower_arm", "basket_right_side", "0"),
    ("right_hand", "basket_right_side", "0"),
    ("left_thigh", "root", "3"),
    ("left_shin", "basket_left_side", "1"),
    ("left_foot", "basket_left_side", "1"),
    ("right_thigh", "root", "3"),
    ("right_shin", "basket_right_side", "1"),
    ("right_foot", "basket_right_side", "1")
  ]
}

```

```

Prompt section6: reference example-output
step5: get close to the chair.
{
  human_root_target: chair(front),
  object_root_target: chair(center),
  relative_movement_dynamics:
  [
    ("pelvis", "root", "1"),
    ("torso", "root", "1"),
    ("head", "root", "1"),
    ("left_upper_arm", "root", "1"),
    ("left_lower_arm", "root", "1"),
    ("left_hand", "root", "1"),
    ("right_upper_arm", "root", "1"),
    ("right_lower_arm", "root", "1"),
    ("right_hand", "root", "1"),
    ("left_thigh", "root", "3"),
    ("left_shin", "root", "3"),
    ("left_foot", "root", "3"),
    ("right_thigh", "root", "3"),
    ("right_shin", "root", "3"),
    ("right_foot", "root", "3")
  ]
}

```

```

Prompt section6: reference example-output
step6: sit down.
{
  human_root_target: chair(center),
  object_root_target: chair(center),
  relative_movement_dynamics:
  [
    ("pelvis", "seat_support", "1"),
    ("torso", "root", "3"),
    ("head", "root", "3"),
    ("left_upper_arm", "root", "3"),
    ("left_lower_arm", "root", "3"),
    ("left_hand", "root", "3"),
    ("right_upper_arm", "root", "3"),
    ("right_lower_arm", "root", "3"),
    ("right_hand", "root", "3"),
    ("left_thigh", "chair_foot", "0"),
    ("left_shin", "chair_foot", "0"),
    ("left_foot", "chair_foot", "0"),
    ("right_thigh", "chair_foot", "0"),
    ("right_shin", "chair_foot", "0"),
    ("right_foot", "chair_foot", "0")
  ]
}

```

```

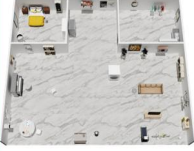
Prompt section6: reference example-output
step7: have a rest.
{
  human_root_target: chair(center),
  object_root_target: chair(center),
  relative_movement_dynamics:
  [
    ("pelvis", "seat_support", "0"),
    ("torso", "back_soft_support", "1"),
    ("head", "head_pillow", "1"),
    ("left_upper_arm", "root", "3"),
    ("left_lower_arm", "left_arm_sofa", "1"),
    ("left_hand", "root", "3"),
    ("right_upper_arm", "root", "3"),
    ("right_lower_arm", "right_arm_sofa", "1"),
    ("right_hand", "root", "3"),
    ("left_thigh", "chair_foot", "0"),
    ("left_shin", "chair_foot", "0"),
    ("left_foot", "chair_foot", "0"),
    ("right_thigh", "chair_foot", "0"),
    ("right_shin", "chair_foot", "0"),
    ("right_foot", "chair_foot", "0")
  ]
}

```

Figure 12. Details of prompt section 6.

Instruction: You are so tired, please take a deep rest.

Top-view image:



```
{
  human_root_target: sofa_bed(front),
  object_root_target: sofa_bed(center),
  relative_movement_dynamics: [
    ("pelvis", "root", "1"),
    ("torso", "root", "1"),
    ("head", "root", "1"),
    ("left_upper_arm", "root", "1"),
    ("left_lower_arm", "root", "1"),
    ("left_hand", "root", "1"),
    ("right_upper_arm", "root", "1"),
    ("right_lower_arm", "root", "1"),
    ("right_hand", "root", "1"),
    ("left_thigh", "root", "3"),
    ("left_shin", "root", "3"),
    ("left_foot", "root", "3"),
    ("right_thigh", "root", "3"),
    ("right_shin", "root", "3"),
    ("right_foot", "root", "3")
  ]
}
```



Instruction: You are so tired, please take a deep rest.

Top-view image:



```
{
  human_root_target: sofa_bed(center),
  object_root_target: sofa_bed(center),
  relative_movement_dynamics: [
    ("pelvis", "seat_cushion", "1"),
    ("torso", "seat_cushion", "1"),
    ("head", "left_armrest", "1"),
    ("left_upper_arm", "root", "3"),
    ("left_lower_arm", "root", "3"),
    ("left_hand", "root", "3"),
    ("right_upper_arm", "root", "3"),
    ("right_lower_arm", "root", "3"),
    ("right_hand", "root", "3"),
    ("left_thigh", "root", "3"),
    ("left_shin", "root", "3"),
    ("left_foot", "right_armrest", "1"),
    ("right_thigh", "root", "3"),
    ("right_shin", "root", "3"),
    ("right_foot", "right_armrest", "1")
  ]
}
```



Figure 13. Visualization of long-term interaction with objects in an indoor home setting (part 1).

Instruction: You are so tired, please take a deep rest.

Top-view image:



step3: Get up and leave.

```
{
  human_root_target: TV_stand(left),
  object_root_target: sofa_bed(center),
  relative_movement_dynamics:
  [
    ["pelvis", "seat_cushion", "2"],
    ["torso", "seat_cushion", "2"],
    ["head", "left_armrest", "2"],
    ["left_upper_arm", "root", "3"],
    ["left_lower_arm", "root", "3"],
    ["left_hand", "root", "3"],
    ["right_upper_arm", "root", "3"],
    ["right_lower_arm", "root", "3"],
    ["right_hand", "root", "3"],
    ["left_thigh", "root", "3"],
    ["left_shin", "root", "3"],
    ["left_foot", "right_armrest", "2"],
    ["right_thigh", "root", "3"],
    ["right_shin", "root", "3"],
    ["right_foot", "right_armrest", "2"]
  ]
}
```



Instruction: Set up for clothes washing.

Top-view image:



step1: Get close to the washing machine.


```
{
  human_root_target: washing_machine(front),
  object_root_target: washing_machine(center),
  relative_movement_dynamics:
  [
    ["pelvis", "root", "1"],
    ["torso", "root", "1"],
    ["head", "root", "1"],
    ["left_upper_arm", "root", "1"],
    ["left_lower_arm", "root", "1"],
    ["left_hand", "root", "1"],
    ["right_upper_arm", "root", "1"],
    ["right_lower_arm", "root", "1"],
    ["right_hand", "root", "1"],
    ["left_thigh", "root", "3"],
    ["left_shin", "root", "3"],
    ["left_foot", "root", "3"],
    ["right_thigh", "root", "3"],
    ["right_shin", "root", "3"],
    ["right_foot", "root", "3"]
  ]
}
```



Figure 14. Visualization of long-term interaction with objects in an indoor home setting (part 2).

Instruction: Set up for clothes washing.

Top-view image:




```


step2: Push the washing machine.
{
  human_root_target: black&white_paintings(front),
  object_root_target: black&white_paintings(front),
  relative_movement_dynamics:
  {
    ["pelvis", "root", "0"],
    ["torso", "root", "0"],
    ["head", "root", "0"],
    ["left_upper_arm", "root", "3"],
    ["left_lower_arm", "root", "3"],
    ["left_hand", "control_panel", "0"],
    ["right_upper_arm", "root", "3"],
    ["right_lower_arm", "root", "3"],
    ["right_hand", "soap_dispenser", "0"],
    ["left_thigh", "root", "3"],
    ["left_shin", "root", "3"],
    ["left_foot", "root", "3"],
    ["right_thigh", "root", "3"],
    ["right_shin", "root", "3"],
    ["right_foot", "root", "3"]
  }
}

```



Instruction: Set up for clothes washing.

Top-view image:




```

step3: Leave the washing machine.
{
  human_root_target: tea_chair(back),
  object_root_target: washing_machine(center),
  relative_movement_dynamics:
  {
    ["pelvis", "root", "2"],
    ["torso", "root", "2"],
    ["head", "root", "2"],
    ["left_upper_arm", "root", "3"],
    ["left_lower_arm", "root", "3"],
    ["left_hand", "root", "3"],
    ["right_upper_arm", "root", "3"],
    ["right_lower_arm", "root", "3"],
    ["right_hand", "root", "3"],
    ["left_thigh", "root", "3"],
    ["left_shin", "root", "3"],
    ["left_foot", "root", "3"],
    ["right_thigh", "root", "3"],
    ["right_shin", "root", "3"],
    ["right_foot", "root", "3"]
  }
}

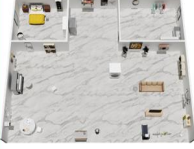
```



Figure 15. Visualization of long-term interaction with objects in an indoor home setting (part 3).

Instruction: The clothes are being washed, you can sit and relax for a while.

Top-view image:



step1: Get close to the tea chair.

```
{
  human_root_target: tea_chair(front),
  object_root_target: tea_chair(center),
  relative_movement_dynamics:
  [
    ("pelvis", "root", "1"),
    ("torso", "root", "1"),
    ("head", "root", "1"),
    ("left_upper_arm", "root", "1"),
    ("left_lower_arm", "root", "1"),
    ("right_upper_arm", "root", "1"),
    ("right_lower_arm", "root", "1"),
    ("right_hand", "root", "1"),
    ("left_thigh", "root", "3"),
    ("left_shin", "root", "3"),
    ("left_foot", "root", "3"),
    ("right_thigh", "root", "3"),
    ("right_shin", "root", "3"),
    ("right_foot", "root", "3")
  ]
}
```



Instruction: The clothes are being washed, you can sit and relax for a while.

Top-view image:



step2: Sit down.

```
{
  human_root_target: tea_chair(center),
  object_root_target: tea_chair(center),
  relative_movement_dynamics:
  [
    ("pelvis", "seat_surface", "1"),
    ("torso", "backrest", "1"),
    ("head", "root", "3"),
    ("left_upper_arm", "root", "3"),
    ("left_lower_arm", "root", "3"),
    ("left_hand", "left_armrest", "1"),
    ("right_upper_arm", "root", "3"),
    ("right_lower_arm", "root", "3"),
    ("right_hand", "right_armrest", "1"),
    ("left_thigh", "root", "3"),
    ("left_shin", "root", "3"),
    ("left_foot", "root", "3"),
    ("right_thigh", "root", "3"),
    ("right_shin", "root", "3"),
    ("right_foot", "root", "3")
  ]
}
```

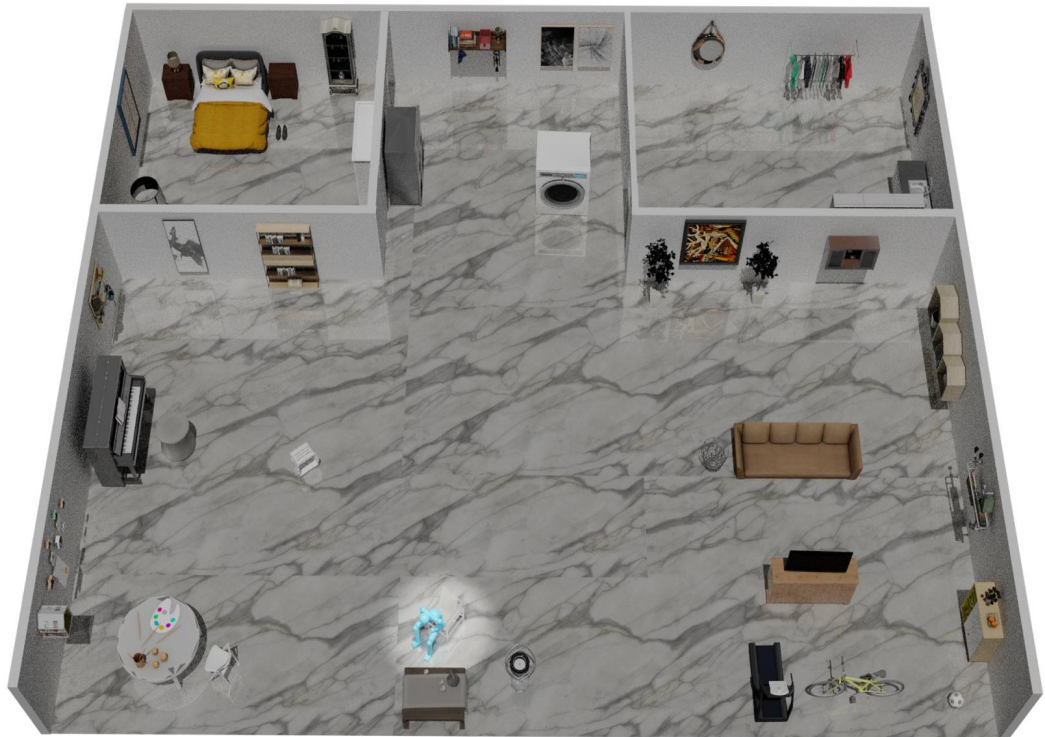


Figure 16. Visualization of long-term interaction with objects in an indoor home setting (part 4).

Instruction: The clothes are being washed, you can sit and relax for a while.

Top-view image:



step3: Stand up and leave.

```
{
  human_root_target: tea_desk(front),
  object_root_target: tea_chair(center),
  relative_movement_dynamics:
  [
    ("pelvis", "seat_surface", "2"),
    ("torso", "backrest", "2"),
    ("head", "root", "3"),
    ("left_upper_arm", "root", "3"),
    ("left_lower_arm", "root", "3"),
    ("left_hand", "left_armrest", "2"),
    ("right_upper_arm", "root", "3"),
    ("right_lower_arm", "root", "3"),
    ("right_hand", "right_armrest", "2"),
    ("left_thigh", "root", "3"),
    ("left_shin", "root", "3"),
    ("left_foot", "root", "3"),
    ("right_thigh", "root", "3"),
    ("right_shin", "root", "3"),
    ("right_foot", "root", "3")
  ]
}
```



Instruction: The clothes are ready, please collect them in the basket and hang them to dry.

Top-view image:



step1: Get close to the laundry basket.

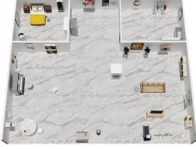
```
{
  human_root_target: laundry_basket(front),
  object_root_target: laundry_basket(center),
  relative_movement_dynamics:
  [
    ("pelvis", "root", "1"),
    ("torso", "root", "1"),
    ("head", "root", "1"),
    ("left_upper_arm", "basket_left_side", "1"),
    ("left_lower_arm", "basket_left_side", "1"),
    ("left_hand", "basket_left_side", "1"),
    ("right_upper_arm", "basket_right_side", "1"),
    ("right_lower_arm", "basket_right_side", "1"),
    ("right_hand", "basket_right_side", "1"),
    ("left_thigh", "root", "3"),
    ("left_shin", "root", "3"),
    ("left_foot", "root", "3"),
    ("right_thigh", "root", "3"),
    ("right_shin", "root", "3"),
    ("right_foot", "root", "3")
  ]
}
```



Figure 17. Visualization of long-term interaction with objects in an indoor home setting (part 5).

Instruction: The clothes are ready, please collect them in the basket and hang them to dry.

Top-view image:



step2: Squat down and pick up the laundry basket.

```

human_root_target: laundry basket(front),
object_root_target: laundry basket(center),
relative_movement_dynamics:
{
  ["pelvis", "root", "1"],
  ["torso", "root", "1"],
  ["head", "root", "1"],
  ["left_upper_arm", "basket_left_side", "0"],
  ["left_lower_arm", "basket_left_side", "0"],
  ["left_hand", "basket_left_side", "0"],
  ["right_upper_arm", "basket_right_side", "0"],
  ["right_lower_arm", "basket_right_side", "0"],
  ["right_hand", "basket_right_side", "0"],
  ["left_thigh", "root", "3"],
  ["left_shin", "basket_left_side", "2"],
  ["left_foot", "basket_left_side", "2"],
  ["right_thigh", "root", "3"],
  ["right_shin", "basket_right_side", "2"],
  ["right_foot", "basket_right_side", "2"]
}

```



Instruction: The clothes are ready, please collect them in the basket and hang them to dry.

Top-view image:



step3: Walking to the washing machine while holding the laundry basket.

```

human_root_target: washing machine(front),
object_root_target: washing machine(front),
relative_movement_dynamics:
{
  ["pelvis", "root", "0"],
  ["torso", "root", "0"],
  ["head", "root", "0"],
  ["left_upper_arm", "basket_left_side", "0"],
  ["left_lower_arm", "basket_left_side", "0"],
  ["left_hand", "basket_left_side", "0"],
  ["right_upper_arm", "basket_right_side", "0"],
  ["right_lower_arm", "basket_right_side", "0"],
  ["right_hand", "basket_right_side", "0"],
  ["left_thigh", "root", "3"],
  ["left_shin", "root", "3"],
  ["left_foot", "root", "3"],
  ["right_thigh", "root", "3"],
  ["right_shin", "root", "3"],
  ["right_foot", "root", "3"]
}

```



Figure 18. Visualization of long-term interaction with objects in an indoor home setting (part 6).

Instruction: The clothes are ready, please collect them in the basket and hang them to dry.

Top-view image:



step4: Put down the laundry basket to collect clothes.

```
{
  human_root_target: washing machine(front),
  object_root_target: washing machine(front),
  relative_movement_dynamics:
  {
    ["pelvis", "root", "2"],
    ["torso", "root", "2"],
    ["head", "root", "2"],
    ["left_upper_arm", "basket_left_side", "0"],
    ["left_lower_arm", "basket_left_side", "0"],
    ["left_hand", "basket_left_side", "0"],
    ["right_upper_arm", "basket_right_side", "0"],
    ["right_lower_arm", "basket_right_side", "0"],
    ["right_hand", "basket_right_side", "0"],
    ["left_thigh", "root", "3"],
    ["left_shin", "basket_left_side", "1"],
    ["left_foot", "basket_left_side", "1"],
    ["right_thigh", "root", "3"],
    ["right_shin", "basket_right_side", "1"],
    ["right_foot", "basket_right_side", "1"]
  }
}
```



Instruction: The clothes are ready, please collect them in the basket and hang them to dry.

Top-view image:



step5: Pick up the laundry basket after collecting clothes.

```
{
  human_root_target: laundry basket(front),
  object_root_target: laundry basket(center),
  relative_movement_dynamics:
  {
    ["pelvis", "root", "1"],
    ["torso", "root", "1"],
    ["head", "root", "1"],
    ["left_upper_arm", "basket_left_side", "0"],
    ["left_lower_arm", "basket_left_side", "0"],
    ["left_hand", "basket_left_side", "0"],
    ["right_upper_arm", "basket_right_side", "0"],
    ["right_lower_arm", "basket_right_side", "0"],
    ["right_hand", "basket_right_side", "0"],
    ["left_thigh", "root", "3"],
    ["left_shin", "basket_left_side", "2"],
    ["left_foot", "basket_left_side", "2"],
    ["right_thigh", "root", "3"],
    ["right_shin", "basket_right_side", "2"],
    ["right_foot", "basket_right_side", "2"]
  }
}
```



Figure 19. Visualization of long-term interaction with objects in an indoor home setting (part 7).

Instruction: The clothes are ready, please collect them in the basket and hang them to dry.

Top-view image:



steps: Walking to the drying rack while holding the laundry basket.

```
human_root_target: drying rack(front),
object_root_target: drying rack(front),
relative_movement_dynamics:
[
  ["pelvis", "root", "0"],
  ["torso", "root", "0"],
  ["head", "root", "0"],
  ["left_upper_arm", "basket_left_side", "0"],
  ["left_lower_arm", "basket_left_side", "0"],
  ["left_hand", "basket_left_side", "0"],
  ["right_upper_arm", "basket_right_side", "0"],
  ["right_lower_arm", "basket_right_side", "0"],
  ["right_hand", "basket_right_side", "0"],
  ["left_thigh", "root", "3"],
  ["left_shin", "root", "3"],
  ["left_foot", "root", "3"],
  ["right_thigh", "root", "3"],
  ["right_shin", "root", "3"],
  ["right_foot", "root", "3"]
]
```



Figure 20. Visualization of long-term interaction with objects in an indoor home setting (part 8).